

Evan Ruzanski*
Vaisala, Inc., Louisville, Colorado

V. Chandrasekar
Colorado State University, Fort Collins, Colorado

1. INTRODUCTION

Nowcasting precipitation has traditionally been done using radar reflectivity data. Recent research, however, indicates that using specific differential phase (K_{dp}) has several advantages over using reflectivity for estimating rainfall. This paper presents an evaluation of nowcasting rainfall fields based on K_{dp} estimates using the Collaborative Adaptive Sensing of the Atmosphere (CASA) quantitative precipitation estimation and nowcasting methodologies and approximately 27 h of composite X-band radar data. The results show the predictability of K_{dp} -based rainfall estimates to be about twice that of reflectivity-based rainfall estimates in terms of cross-correlation and equitable threat score considering radar-based estimates as the scoring reference. The benefits of quantitative precipitation nowcasting using K_{dp} -based estimates were shown to diminish with increasing lead time out to 20 min when considering rain gauge cross-validation.

2. RAINFALL ESTIMATION USING SPECIFIC DIFFERENTIAL PHASE

Specific differential phase (K_{dp}), defined as one-half the range (r) derivative of the two-way differential phase (Φ_{dp}),

$$K_{dp} = \frac{1}{2} \frac{d\Phi_{dp}(r)}{dr} \quad (1)$$

has several advantages over using reflectivity for estimating rainfall (Seliga and Bringi 1978; Jameson 1985; Bringi and Chandrasekar 2001). Since Φ_{dp} is a dual-polarized radar product and not a power measurement, rainfall estimates derived from K_{dp} are not susceptible to radar calibration error, attenuation, or beam blockage and are less affected by anomalous propagation (Brandes et al. 2001). K_{dp} -based rainfall estimates are also less sensitive to variations in drop size distributions (Sachidananda and Znić 1987) and to the presence of dry, tumbling hail (Balakrishnan and Znić 1990; Aydin et al. 1995).

The estimation of K_{dp} involves approximating the slope of Φ_{dp} profiles, which is known to be a noisy and unstable computation. Methods for estimating K_{dp}

traditionally involved piecewise fitting to predict the local trend, where any phase sample deviating too far from this trend was attributed to phase wrapping. Approaches were developed to then reduce the variance of K_{dp} estimates, including range filtering, linear fitting, or both (Golestani et al. 1989; Hubbert et al. 1993). These techniques reduce the peak estimated K_{dp} values, which can introduce bias, and afford limited adaptive capability to follow steep slopes within intense rain cells and reduce the estimation variance in the rest of the segments simultaneously.

Wang and Chandrasekar (2009) presented an adaptive scheme to estimate K_{dp} , which was shown to have better range resolution in intense rain cells to better capture small-scale variability. A regularization technique is used to control the balance between estimation bias and variance and incorporates adaptivity to keep up with large gradients of Φ_{dp} . Wang and Chandrasekar (2009) showed K_{dp} fields estimated using this approach matched the structure of a single storm observed by the CASA X-band radar network better than previous approaches and that negative K_{dp} values were largely eliminated. Wang and Chandrasekar (2010) showed K_{dp} -based rainfall estimates using this method compared favorably to rain gauge measurements.

3. NOWCASTING METHODOLOGY

The Dynamic and Adaptive Radar Tracking of Storms (DARTS) nowcasting model (Ruzanski et al. 2010) was used to estimate motion between sequences of estimated rainfall fields. DARTS is built upon the general continuity equation describing the flux and evolution of a precipitation pattern represented by a temporal sequence of radar reflectivity fields, $F(x, y, t)$, given by,

$$\begin{aligned} \frac{\partial}{\partial t} F(x, y, t) = & -U(x, y) \frac{\partial}{\partial x} F(x, y, t) \\ & -V(x, y) \frac{\partial}{\partial y} F(x, y, t) \end{aligned} \quad (2)$$

where $U(x, y)$ is the east-west component of the velocity field and $V(x, y)$ is the north-south component of the velocity field. DARTS estimates precipitation pattern motion by representing Eq (2) as a discrete spatiotemporal linear model, where the Discrete Fourier Transform coefficients of $U(x, y)$ and $V(x, y)$ are estimated using linear least squares estimation

* *Corresponding author address:* Evan Ruzanski, Vaisala, Inc., Boulder Operations, Louisville, CO 80027; e-mail: evan.ruzanski@vaisala.com.

(Ruzanski et al. 2010). Advection is performed using a sinc kernel-based method described by Ruzanski et al. (2010).

4. DATA

Approximately 27 h of data (1593 data frames) collected during the 2009 CASA IP1 experiment (Brotzge et al. 2005) were used for evaluation [Table 1]. Data were collected from 2-degree scans and projected and merged onto Plan Position Indicator (PPI) grids with 0.5 km spacing using the technique described by Liu et al. (2007). The temporal resolution of the data is 1 min.

Rainfall rate fields (R) were estimated from K_{dp} according to (Wang and Chandrasekar 2010),

$$R = 18.15K_{dp}^{0.791} \quad (3)$$

where K_{dp} has units of degree km^{-1} and R has units of mm h^{-1} . The convective (non-tropical) or “default” Z - R relationship currently used by WSR-88D radars (Fulton et al. 1998),

$$Z = 300R^{1.4} \quad (4)$$

where Z has units of $\text{mm}^6 \text{m}^{-3}$ and R has units of mm h^{-1} , was used to create the reflectivity-based rainfall estimates as a reference for assessing the nowcasting characteristics of K_{dp} -based rainfall estimates.

Rain gauge cross-validation was performed using data collected by gauges located within the Little Washita River Experimental Watershed (LWREW), which is managed by the U. S. Department of Agriculture (USDA) Agricultural Research Service (ARS) as part of the Little Washita Micronetwork (Allen and Naney 1991). The LWREW covers an area of 611 km^2 and is situated in the center of the CASA IP1 test bed allowing for overlapping coverage from almost all the CASA IP1 radars (Figure 1). Data from 20 unheated tipping-bucket rain gauges deployed within the watershed were considered, which measure rainfall in discrete bucket tips of 0.254 mm per tip. The gauge data were archived as running rainfall accumulation in 5-min intervals over a 24-h period. Piecewise Cubic Hermite Interpolating Polynomial derivation was used to temporally align the radar and gauge data and estimate rainfall rate from measured accumulation (Fritsch and Carlson 1980).

5. ASSESSMENT METHODOLOGY

Nowcasting performance was assessed considering radar-based estimates and rain gauge observations as reference for predicted rainfall fields. In operational use, the particular K_{dp} - R and Z - R relationships used will cause large differences in rainfall estimates (Anagnostou and Krajewski 1998).

Table 1. Summary of precipitation event data collected during the 2009 CASA IP1 experiment used for nowcasting performance evaluation.

Event no.	Start time	Duration (h)	Type
1	0015 UTC 10 Mar	4.75	Line
2	0027 UTC 31 Mar	2.20	Line
3	0858 UTC 02 May	6.75	Multicell
4	1423 UTC 05 May	3.15	Multicell
5	0907 UTC 11 May	5.85	Multicell
6	0200 UTC 14 May	5.75	Supercell

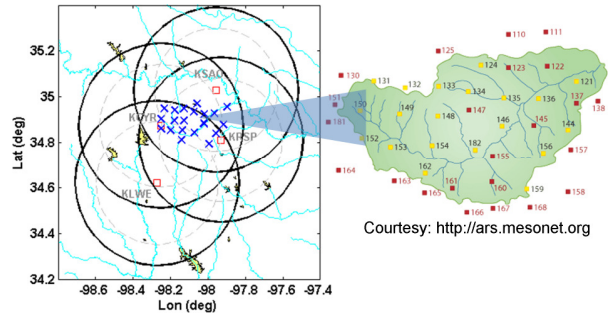


Figure 1. The distribution of ARS Micronet gauge network within the IP1 network coverage area. A current operational gauge station is denoted by an ‘x’ on the left and labeled with station IDs on the right [from Wang and Chandrasekar (2010)].

Because validation of radar-based rainfall estimates is a difficult problem in itself and methods of uncertainty determination are not well established (Ciach and Krajewski 1999; Anagnostou and Krajewski 1999), nowcasting assessment was performed relative to radar-based rainfall estimates in addition to rain gauge cross-validation.

The cross-correlation coefficient (CC) and Equitable Threat Score (ETS) were used to assess nowcasting performance relative to radar-based rainfall intensity estimates. The CC is defined as,

$$CC = \frac{\sum_{i=1}^N O_i F_i}{\left[\sum_{i=1}^N O_i^2 \right]^{0.5} \left[\sum_{i=1}^N F_i^2 \right]^{0.5}} \quad (5)$$

where N is the total number of 0-min rainfall estimates, O , and forecasts, F , in the estimated rainfall field corresponding to each respective rainfall estimator.

The ETS is defined as,

$$ETS = \frac{A - A_R}{A + B + C - A_R} \quad (6)$$

where A represents the intersection of the areas in the data field over which the event was forecast and subsequently occurred (i.e., “hit”), B represents the area over which the event was forecast and subsequently did not occur (i.e., “false alarm”), C represents the area over which the event occurred but was not forecast to occur (i.e., “miss”), D represents the intersection of the areas over which the event was not forecast to occur and did not occur (i.e., “correct negative”), and A_R is an estimate of the number of hits due to random chance, given by,

$$A_R = \frac{(A+B)(A+C)}{A+B+C+D} \quad (7)$$

In this study, an “event” is defined as the presence of a rainfall value greater than or equal to 5 mm h^{-1} located within a $1 \text{ km} \times 1 \text{ km}$ area.

Normalized Bias (NB), Normalized Standard Error (NSE), and the CC were used to assess nowcasting characteristics of 1-h rainfall accumulation fields relative to rain gauge observations. The NB and NSE are defined respectively as,

$$\text{NB} = \frac{\langle R_R - R_G \rangle}{\langle R_G \rangle} \quad (8)$$

and

$$\text{NSE} = \frac{\langle |R_R - R_G| \rangle}{\langle R_G \rangle} \quad (9)$$

where R_R is the radar estimate, R_G is the gauge observation, and the brackets indicate the sample (spatial) average. The CC is defined in Eq (5) and computed between radar measurements chosen at the location of rain gauges and the rain gauge observations temporally interpolated to the time of the estimated or predicted rain rate fields.

6. RESULTS

Example rainfall rate fields estimated using Eqs (3) and (4) and corresponding 10-min predicted rain rate fields from the 31 Mar event are shown in Figure 2. This figure depicts the variability in the structure of rainfall fields estimated by K_{dp} and reflectivity and their predictions.

The average MAE, ETS, and CC scores considering radar-based rainfall estimates as the reference are shown in Figure 3. The results show that rainfall fields estimated from K_{dp} exhibit higher ETS and CC values with increasing lead time vs rainfall estimated from reflectivity.

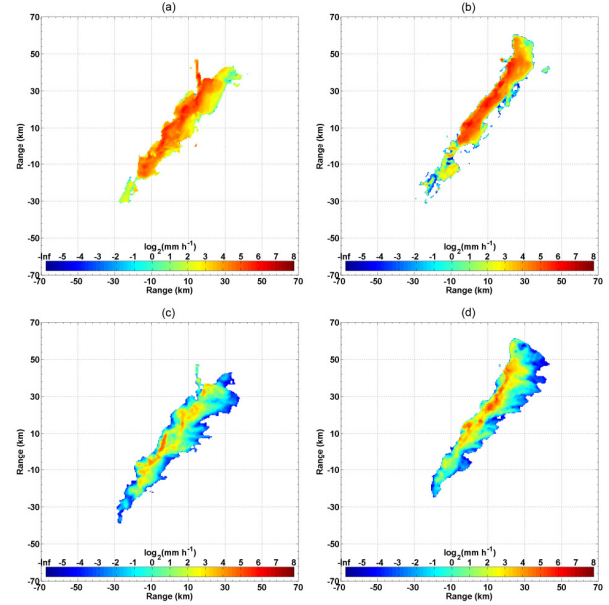


Figure 2. Rain rate fields corresponding to 0055 UTC 31 Mar 2009: (a) initial estimate and (b) corresponding 10-min prediction of rainfall field derived according to Eq (3), (c) initial estimate and (d) corresponding 10-min prediction of rainfall field derived according to Eq (4).

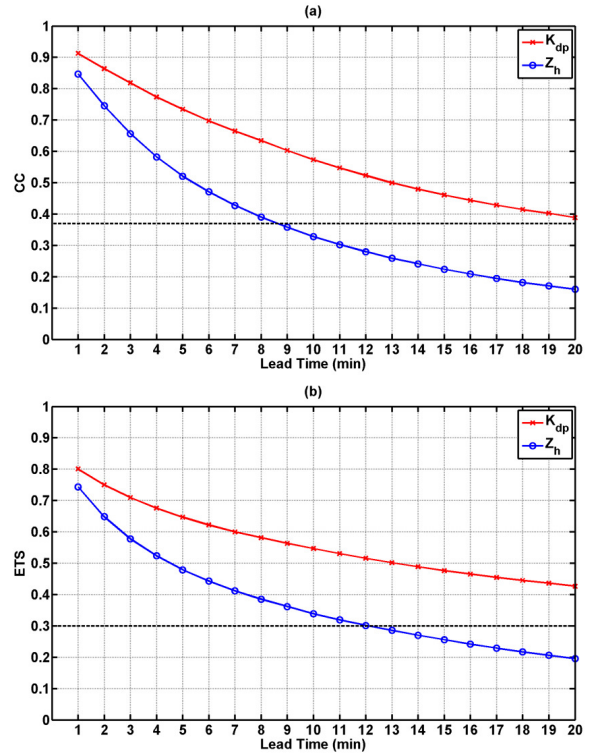


Figure 3. Comparison of nowcasting performance using (a) CC, and (b) ETS scores and radar-based estimates as scoring reference.

Using values of $ETS = 0.3$ and $CC = 1/e$ as estimates of predictability (Germann and Zawadzki 2002), the predictability of K_{dp} -based rainfall estimates is shown to be approximately twice that of reflectivity-based estimates using radar-based rainfall estimates as the scoring reference.

The average NB, CC, and NSE scores considering rain gauge observations as the scoring reference are shown in Figure 4. Figure 4 shows K_{dp} -based rainfall estimates to be more positively biased (with less overall bias) vs reflectivity-based estimates throughout the nowcast period, with all biases decreasing with increasing lead time. The CC is shown to be higher for K_{dp} -based rainfall estimates vs reflectivity-based estimates throughout the nowcast period suggesting more coherence in the K_{dp} -based rainfall estimates with increasing lead time. NSE scores are also shown to be lower throughout the nowcast period for K_{dp} -based rainfall estimates vs reflectivity-based estimates. Collectively, these results suggest the benefits of using K_{dp} for quantitative precipitation estimation diminish with increasing lead time.

7. CONCLUSIONS AND FUTURE WORK

Estimating rainfall from K_{dp} has several advantages over using reflectivity. K_{dp} estimates are not susceptible to radar calibration error, attenuation, or beam blockage and are less affected by anomalous propagation. Rainfall estimates derived from K_{dp} are also less sensitive to variations in drop size distributions and to the presence of dry, tumbling hail than those derived from reflectivity.

This paper presented a study assessing the characteristics of nowcasting rainfall fields derived from K_{dp} using the method presented by Wang and Chandrasekar (2009). This method has been shown to produce more accurate and robust estimates than previous methods to estimate K_{dp} . Approximately 27 h of X-band radar data collected during the 2009 CASA IP1 experiment was considered for evaluation and the CASA nowcasting methodology was used to generate predictions of K_{dp} - and reflectivity-derived rainfall products out to 20 min. Continuous and categorical scores were used to assess nowcasts relative to their respective radar-based estimates and rain gauge observations. The results showed that the predictability of rainfall fields derived from K_{dp} was about twice that of reflectivity-based estimates in continuous and categorical senses. The scores based on rain gauge cross-validation suggested the benefits of using K_{dp} for quantitative precipitation estimation diminish with increasing lead time. Overall, these results illustrate the potential for improving quantitative precipitation forecasting using K_{dp} -based rainfall estimates.

Future work should consider comparison of K_{dp} -based rainfall estimates to reflectivity-based rainfall fields derived from a collection of several Z-R relationships. A larger data set and various geographic locations should be considered as well.

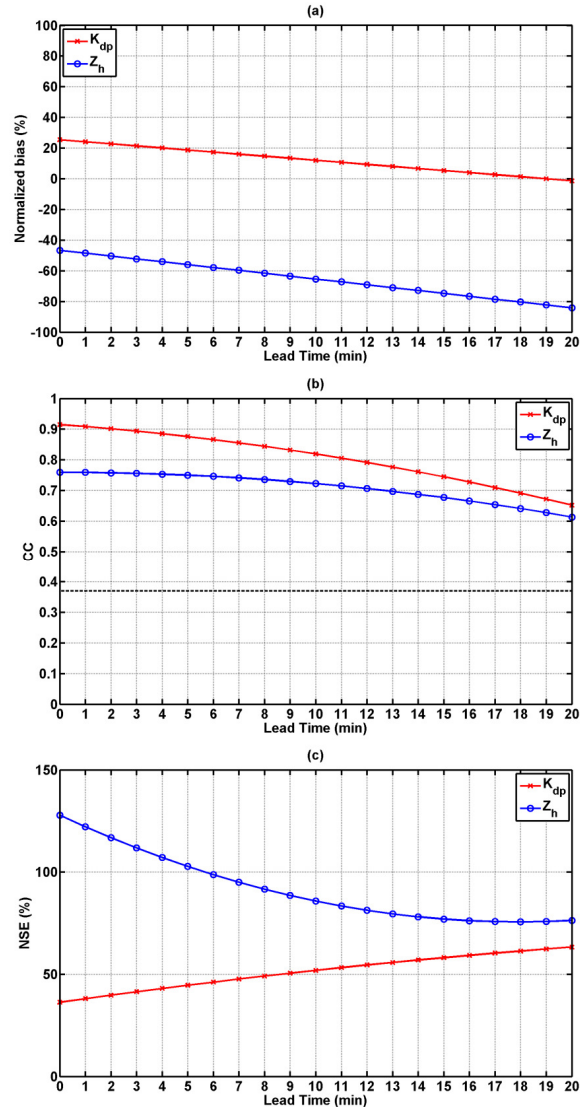


Figure 4. Comparison of nowcasting performance using (a) NB, (b) CC, and (c) NSE scores and rain gauge observations as scoring reference.

Acknowledgement. This work was supported by the Engineering Research Center Program of the National Science Foundation under NSF award number 0313747.

8. REFERENCES

- Allen, P. B., and J. W. Naney, 1991: Hydrology of the Little Washita River Watershed, Oklahoma: Data and analyses. U.S. Department of Agriculture, Agricultural Research Service Publication ARS-90, 73 pp.
- Anagnostou, E. N. and W. F. Krajewski, 1998: Calibration of the WSR-88D precipitation processing subsystem. *Wea. Forecasting*, **13**, 396–406.

- Anagnostou, E. N. and W. F. Krajewski, 1999: Real-time radar rainfall estimation. Part II: Case study. *J. Atmos. Oceanic Technol.*, **16**, 189–197.
- Aydin, K., V. N. Bringi, and L. Liu, 1995: Rain-rate estimation in the presence of hail using S-band specific differential phase and other radar parameters. *J. Appl. Meteor.*, **34**, 404–410.
- Balakrishnan, N. and D. Zrnić, 1990: Estimation of rain and hail rates in mixed-phase precipitation. *J. Atmos. Sci.*, **47**, 565–583.
- Brandes, E. A., C. E. Ryzhkov, and D. S. Zrnić, 2001: An evaluation of radar rainfall estimates from specific differential phase. *J. Atmos. Oceanic Technol.*, **18**, 363–375.
- Bringi, V. N. and V. Chandrasekar, 2001: *Polarimetric Doppler Weather Radar: Principles and Applications*. Cambridge Press, 662 pp.
- Brotzge, J., K. Brewster, B. Johnson, B. Phillips, M. Preston, D. Westbrook, and M. Zink, 2005: CASA's first test bed: Integrative Project #1. Preprints, *32nd Conf. on Radar Meteorology*, Albuquerque, NM, Amer. Meteor. Soc., 14R2.
- Ciach, J. G. and W. F. Krajewski, 1999: On the estimation of radar rainfall variance. *Adv. Water Resour.*, **22**, 585–595.
- Fritsch, F. N., and R. E. Carlson, 1980: Monotone piecewise cubic interpolation. *SIAM J. Numer. Anal.*, **17**, 238–246.
- Fulton, R., J. Breidenbach, D.-J. Seo, D. Miller, and T. O'Bannon, 1998: The WSR-88D rainfall algorithm. *Wea. Forecasting*, **13**, 377–395.
- Germann, U. and I. Zawadzki, 2002: Scale dependence of the predictability of precipitation from continental radar images. Part I: Description of the methodology. *Mon. Wea. Rev.*, **130**, 2859–2873.
- Golestani, Y., V. Chandrasekar, and V. N. Bringi, 1989: Intercomparison of multiparameter radar measurements. Preprints, *24th Int. Conf. on Radar Meteorology*, Tallahassee, FL, Amer. Meteor. Soc., 309–314.
- Hubbert, J. C., V. Chandrasekar, and V. N. Bringi, 1993: Processing and interpretation of coherent dual-polarized radar measurements. *J. Atmos. Oceanic Technol.*, **10**, 155–164.
- Jameson, A., 1985: Microphysical interpretation of multiparameter radar measurements in rain. Part III: Interpretation and measurement of propagation differential phase shift between orthogonal linear polarizations. *J. Atmos. Sci.*, **42**, 607–614.
- Liu, Y., V. Chandrasekar, and V. N. Bringi, 2007: Real-time three-dimensional radar mosaic in CASA IP1 testbed. *Proc. 2007 IEEE Int. Geoscience and Remote Sensing Symp.*, Barcelona, Spain, IEEE, 2754–2757.
- Ruzanski, E., V. Chandrasekar, and Y. Wang, 2011: The CASA nowcasting system. *J. Atmos. Oceanic Technol.*, **28**, 640–655.
- Sachidananda, M. and D. Zrnić, 1987: Rain rate estimates from differential polarization estimates. *J. Atmos. Oceanic Technol.*, **4**, 588–598.
- Seliga, T. A. and V. N. Bringi, 1978: Differential reflectivity and differential phase shift: Applications in radar meteorology. *Radio Sci.*, **13**, 271–275.
- Wang, Y. T. and V. Chandrasekar, 2009: Algorithm for estimation of specific differential phase. *J. Atmos. Oceanic Technol.*, **26**, 2565–2578.
- Wang, Y. T. and V. Chandrasekar, 2010: Quantitative precipitation estimation in the CASA X-band dual-polarization radar network. *J. Atmos. Oceanic Technol.*, **27**, 1665–1676.